Deep Learning-Based Histopathological Segmentation Differntiates Cavitation Patterns in Knee and Digit Joints

Minwook Kim[1], Heejong Kim[2], Ben Garcia[3], Wookjin Choi[4]
[1]Rowan-Virtua School of Translational Biomedical Engineering and Sciences, Stratford, NJ,
[2]University of Pennsylvania, Philadelphia, PA, [3]Washington University in St. Louis, St. Louis, MO, [4]Thomas Jefferson University, Philadelphia, PA.
kimmin@rowan.edu

Disclosures: No disclosures

INTRODUCTION: Joint cavitation is a developmental process to create a fluid-filled joint cavity, permitting unhindered joint motion[1]. Our recent study showed that dense fibroblast-like mesenchymal cells in the interzone produce a robust matrix (pericellular coat), mostly hyaluronan (HA)[2]. Cavitation initiates with the appearance of microcavities between cells. The microcavities accumulate, coalesce, and eventually form a single cavity. This physical separation involves HA cleavage into its fragments by hyaluronidase, in turn reducing cell-matrix interactions. While all synovial joints undergo this process, the cavitation timing and patterns are distinct in the knee and digit joints. For instance, cavitation starts and ends within 6-12h (E15-E15.5) in knee joints, where digits take 72-84h (E15-E18.5). Interestingly, the growing femur and tibia progressively flexed (angulated) at the knee during cavitation, but the digit joint changed minimally. Further, the knee interzone cells undergoing cavitation show highly stretched and elongated cell nuclei. In contrast, those in digits remain round, suggesting joint cavitation is differentially regulated in knees and digits. However, what originates such distinct timing and patterns in knee and digit cavitation is unknown. In this study, we used a deep learning technique to identify the potential factor(s) differentially impacting cavitation timing and patterns by learning the spatiotemporal cavitation process using histological data sets.

METHODS: All animal procedures were approved by Rowan University IACUC. To control timed pregnancy, mice were mated overnight and separated in the morning (6 pm – 9 am), and noon on the day of separation was considered E0.5. To determine the cavitation process in knee and digit joints, CD-1 mouse hindlimbs (E14.5 – E18.5 at 12-24h intervals) were collected, embedded in paraffin, sectioned (6μm), and stained with Alcian blue. A nuclear aspect ratio of cavitating interzone cells in knees and digits was quantified using ImageJ software at E15.25 and E18.5 (n=100/group). Unsupervised segmentation (unlabeled regions of interest, ROIs) and autoencoder (AE)-based classification were utilized to classify differences in cavitation patterns in knees and digits using Alcian blue-stained images (n=20-30 images/group). Each image was divided into 256 x 256 (pixel) patches, and a convolutional neural network (CNN)-based unsupervised segmentation was used to identify ROIs. These patches were subsequently fed into a CNN-based AE whose latent space layer was connected to a classifier for input patch classification. The AE was trained using the ROIs identified by the unsupervised segmentation, and the image classes were used to train the classifier. Whole image classifications were determined by maximum voting of the patch results and evaluated by accuracy. To identify possible regulators, mass spectrometry was performed using embryonic tissues from distinct locations: (a) knee proliferating cartilage = future 'bone'; (b) knee interzone = future 'articular cartilage'; (c) digit proliferating cartilage; and (d) digit interzone. Stages were E14.5 and E18.5 (before and after cavitation, respectively) (n=3/group). Significance was determined by one or two-way ANOVA with Tukey's post hoc ($p<0.05$).

RESULTS: Nuclear aspect ratio in the cavitating knee interzone was 2.3 times greater than in the digit interzone. Unsupervised segmentation differentiated classes and frequencies between knees and digit cavitation patterns **(Fig.1)**. Class histogram demonstrated that the frequency of the entire class identified differences between knees and digits, and even the selected ($p<0.005$) class frequency was able to distinguish them **(Fig.1A)**. Likewise, when the 1024 features in the bottleneck layer were reduced to two latent space variable, the knees and digit cavitation patterns were identified with 95% accuracy as shown in the scatter plot by t-SNE **(Fig.1B)**. Then, the two latent variables were used to distinguish the knee and digit cavitation patterns and created class images **(Fig.1C and 1D)**. Each class was identified with different colors. Non-variable features were recognized as a background (grey). In the knees, the extracellular matrix (ECM) in the proliferating cartilage was identified as two classes (purple and dark red), and the pericellular matrix (PCM) was identified as pink (arrow) **(Fig.1D-1)**. The ECM in the interzone was classified as pink **(Fig.1D-2 and 3)**. The matrix in the meniscus was recognized as dark red, while cells were classified as green **(Fig.1D-4)**. In digits **(Fig.1E and F)**, PCM in proliferating cartilage and interzone was identified as two classes (pink and turquoise), but ECM was not classified (primarily shown in grey) **(Fig.1F-1 and 2)**. ECM in ligament was identified as two classes (dark red and brown) **(Fig.1F-3)**, and skin was classified as green, which overlapped with cells **(Fig.1F-4)**. Conversely, we then recreated an image using the two latent variables to validate the accuracy of the classified segmentation **(Fig.2)**. When making the two latent variables into random variables (Variational AE, VAE), the scatter plot showed that the accuracy in distinguishing knees and digits was 98.2% **(Fig.2A)**. The VAE-based model was able to reconstruct the original image with accurate cell and matrix distributions. However, the image was blurry, and the cell shapes on the cartilage surface were simplified. The cells in the reconstructed image were round, whereas those in the input (original) image were elliptical **(Fig.2B and C)**. Mass spec data showed that levels of GTPase-activating protein (Rabgap1) and Neutriphil2 (Nrp2) were 25 and 20 times greater before (E14.5) than after (E18.5) cavitation, respectively. They were exclusively expressed in knee interzone cartilage tissue but not in digit cartilage interzone.

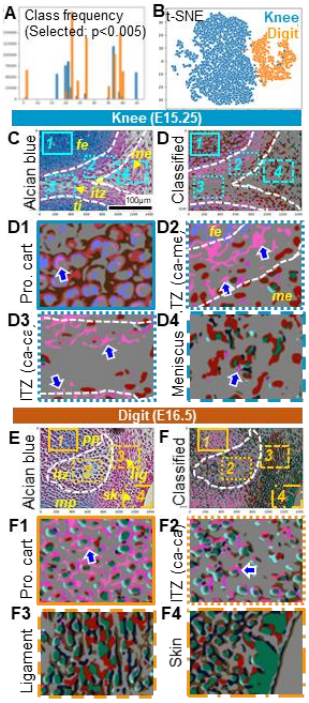

Fig 1. Unsupervised segmentation of cell and matrix in cavitating knees (E15.25) and digits (E16.5). (A) Selected ($p<0.005$) class frequency classification, **(B)** Scatter plot differentiating knees and digits with two potential variables, **(C-F)** Segment-based classification based on the two potential variables.

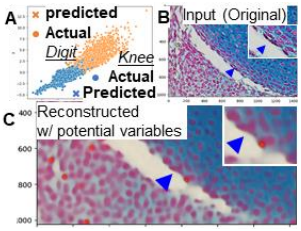

Fig 2. Reconstruction of an image using the identified latent variables. (A) Scatter plot of actual (O) and predicted (X) data sets in knees (blue) and digits (orange). **(B)** Input (raw image sets; Alcain blue stained image). **(C)** Predicted image reconstructed from the two potential variables. (Insets: zoomed images indicating cell morphology).

DISCUSSION: Our data provide new approaches to determining the potential factor(s) in regulating synovial joint cavitation. The unsupervised segmentation identifies relevant ROIs and guides the AE and the classifier to differentiate between knee and digit cavitation patterns even with the two latent variables, indicating that the differences are apparent. Interestingly, a class defined as pink is identified in PCM in proliferating cartilage and ECM in the interzone on both knees and digits. The location expressing the pink class is generally overlapped with HA. However, how the matrix was recognized and used to differentiate them is to be determined. Ligament and skin are identified as green. It may be due to the absence of these tissues in the knee images, so whether this recognition pattern is digit-specific is to be determined. Using the two latent variables, we reconstruct the original image, and it recapitulates most features except for blurriness and cell morphology. We will investigate how the segmentation pattern changes as cell morphology and molecular compositions change with developmental time. Lastly, Rabgap1 and Nrp2 are reported as mechanoresponsive[3-4]. Their spatial expressions, reported role and cell morphology suggest that knee cavitation is in part regulated by biophysical cues, which affect their cavitation timing and patterns.

SIGNIFICANCE/CLINICAL RELEVANCE: This study utilizes deep learning techniques to determine potential factors and whether and how these factors are related to biophysical cues impacting synovial joint cavitation timing and patterns. By developing a deep learning-based segmentation model system using histopathological data, we will provide a novel understanding of how biophysical cues incorporate biological mechanisms in synovial joint development.

REFERENCES: [1] Archer+1999, [2] Kim+2022, [3] Ekpenyong+ 2015, [4] Hoon+ 2016. **ACKNOWLEDGEMENTS:** This work was supported by the NIH (K01 AR078387) and the Rowan-Virtua seed grant.